

## Supporting Information

### **ToF-SIMS Characterization of Surface Chemical Evolution on Electrode Surfaces Educated by Electrochemical Activation**

Jilin Tang<sup>a,b</sup>, Zhigang Ni<sup>c</sup>, Yanyan Zhang<sup>a,\*</sup>, Yao Zhao<sup>a</sup>, Qun Luo<sup>a,b</sup>, Fuyi Wang<sup>a,b,d\*</sup>

<sup>a</sup> Beijing National Laboratory for Molecular Sciences, CAS Key Laboratory of Analytical Chemistry for Living Biosystems, Institute of Chemistry, Chinese Academy of Sciences, Beijing 100190, China

<sup>b</sup> University of Chinese Academy of Sciences, Beijing 100049, China

<sup>c</sup> College of Materials, Chemistry and Chemical Engineering, Hangzhou Normal University, Hangzhou 311121, China

<sup>d</sup> National Centre for Mass Spectrometry in Beijing

\*Correspondence: [zhangyy0816@iccas.ac.cn](mailto:zhangyy0816@iccas.ac.cn); [fuyi.wang@iccas.ac.cn](mailto:fuyi.wang@iccas.ac.cn)

## Experimental Details

### Density functional theory (DFT) calculations

We conducted DFT calculations to optimize the binding geometries of ascorbate on the gold surfaces without or with  $\text{Cl}^-$  (abbreviated as  $\text{Cl}_{\text{ads}}$ ) and to estimate the binding energies (BEs). A two-layer cluster model with 42 and 30 Au atoms on the first and second layers was constructed to simulate the Au surface. Geometry optimizations were performed using the TPSSh functional in combination with the ma-def2-SVP basis set. Grimme's D3 correction augmented with Becke-Johnson (BJ) damping was employed to properly describe the dispersion interactions. The outermost cycle of the Au atoms on the first layer and all Au atoms on the second layer were fixed during the optimization. Electronic energies at the TPSSh-D3BJ/def2-QZVP level were used to obtain more accurate binding energies. Since the def2-QZVP basis set is quite large for DFT methods, basis set superposition error correction is not considered in this work. The solvent effect of water is treated with the CPCM implicit solvation model. All calculations were performed using the ORCA 5.0 program package. The binding energy (BE) was calculated as

$$\text{BE} = E_{\text{ascorbate}} + E_{\text{Au w/o Clads}} - E_{\text{complex}},$$

in which the geometries of ascorbate and gold cluster (with or without  $\text{Cl}_{\text{ads}}$ ) were directly taken from the complex without further optimization.

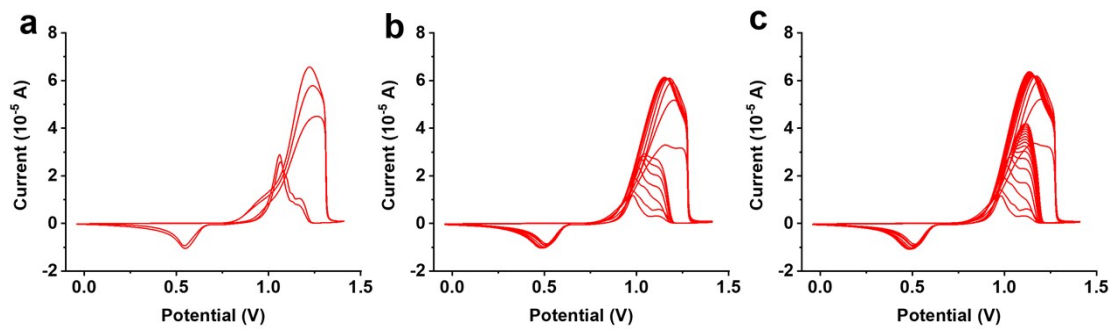


**Figure S1.** CV curves of pretreatment procedure of gold electrode: (a) 5 segments cycling in HCl; (b) 15 segments cycling in HCl; (c) 25 segments cycling in HCl.

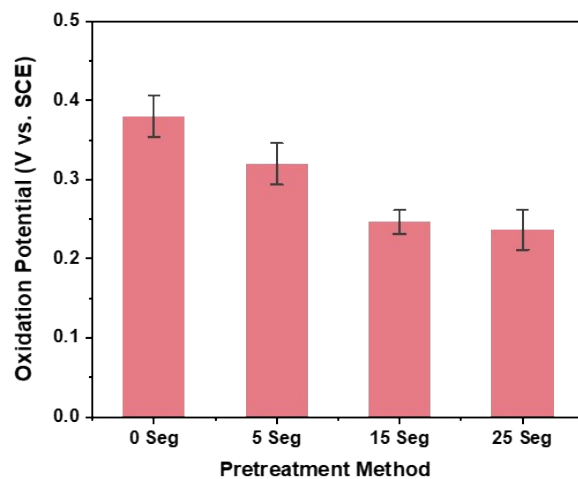


**Figure S2.** The electrochemical oxidation potential of ascorbic acid (5 mM) in 50 mM NaNO<sub>3</sub> solution measured at freshly polished gold electrode before (0 seg) and after being electrochemically treated in 0.37 M HCl solution for 5, 15 or 25 segments. Each group contains three independently prepared gold electrodes.

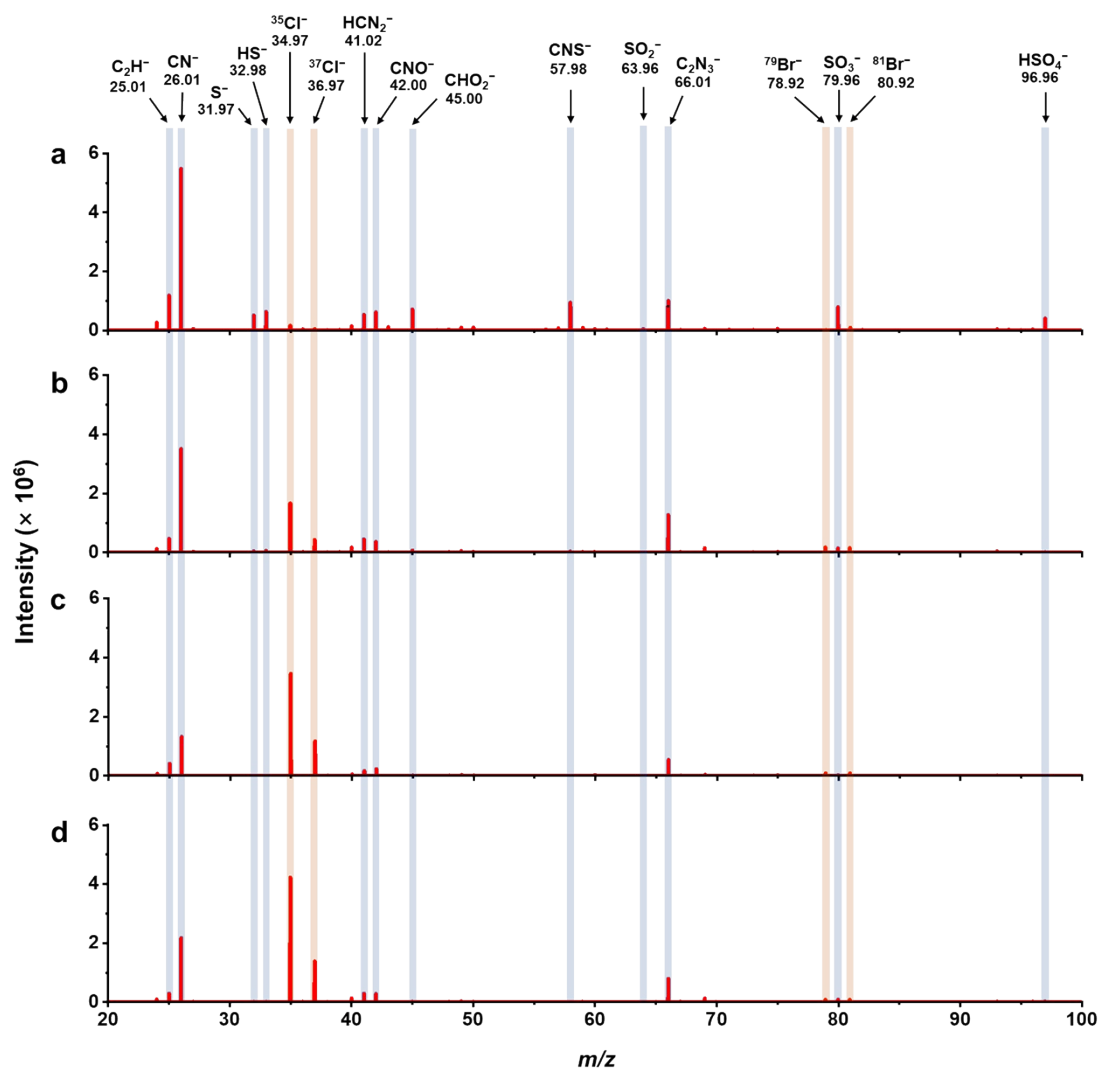


**Figure S3.** The representative ToF-SIMS spectra in the mass range of 20-100 obtained at surfaces of the freshly polished gold electrodes before (a) and after (b-d) being electrochemically treated in 0.37 M HCl for 5 (b), 15 (c), and 25 (d) segments. The signal intensities of ions from surface contaminants including  $C_2H^-$  ( $m/z$  25.01),  $CN^-$  ( $m/z$  26.01),  $S^-$  ( $m/z$  31.97),  $HS^-$  ( $m/z$  32.98),  $HCN_2^-$  ( $m/z$  41.02),  $CNO^-$  ( $m/z$  42.00),  $CHO_2^-$  ( $m/z$  45.00),  $CNS^-$  ( $m/z$  57.98),  $SO_2^-$  ( $m/z$  63.96),  $SO_3^-$  ( $m/z$  79.96), and  $HSO_4^-$  ( $m/z$  96.96) decreased after activation. In comparison, those of  $^{35}Cl^-$  ( $m/z$  34.97) and  $^{37}Cl^-$  ( $m/z$  36.97) ions significantly increased after activation.

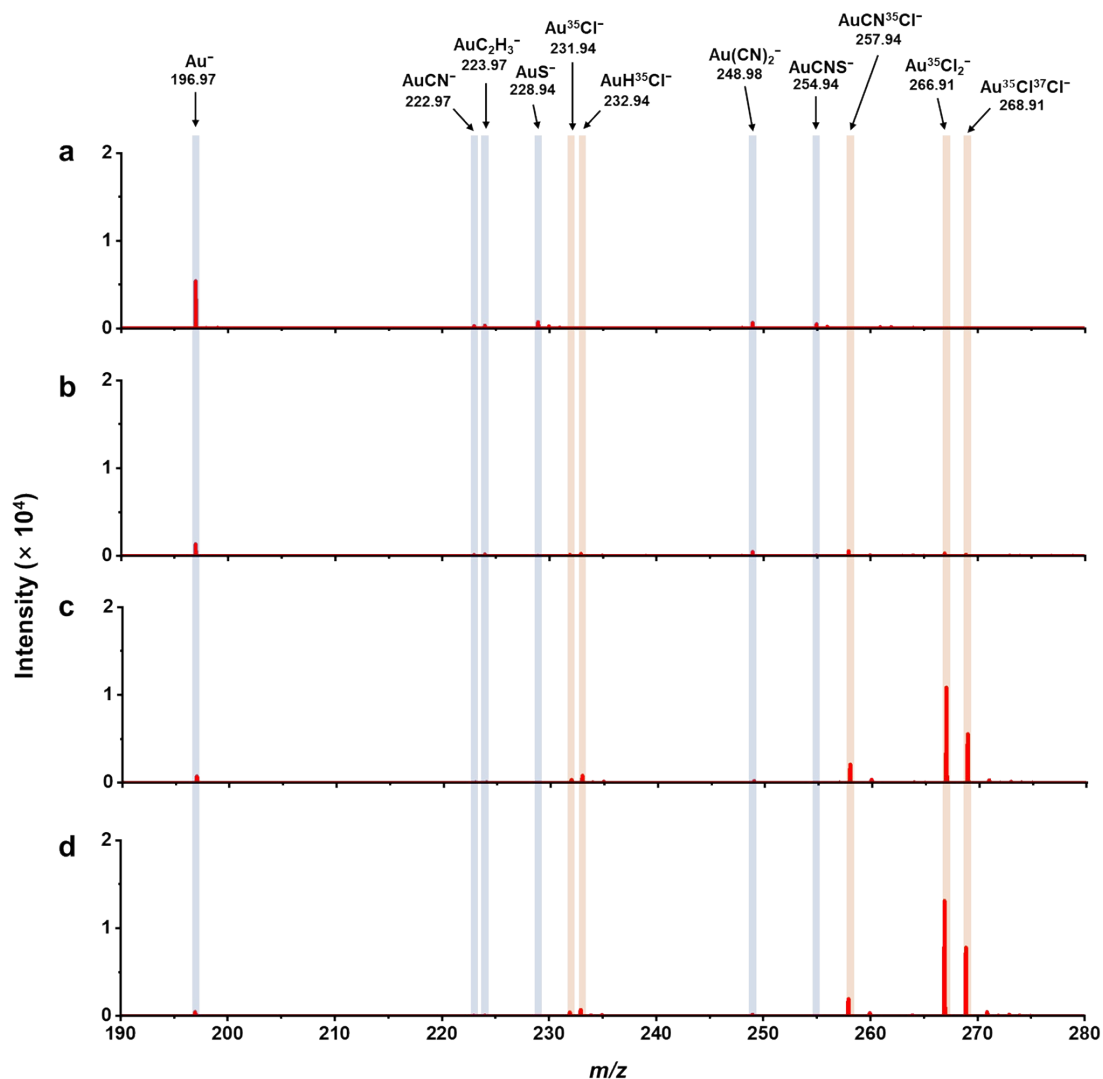


**Figure S4.** The representative ToF-SIMS spectra in the mass range of 190-280 obtained at surfaces of the freshly polished gold electrodes before (a) and after (b-d) being electrochemically treated in 0.37 M HCl for 5 (b), 15 (c), and 25 (d) segments. The signal intensities of  $\text{Au}^-$  ( $m/z$  196.97) ion and ions from surface contaminants including  $\text{AuCN}^-$  ( $m/z$  222.97),  $\text{AuC}_2\text{H}_3^-$  ( $m/z$  223.97),  $\text{AuS}^-$  ( $m/z$  228.94),  $\text{Au}(\text{CN})_2^-$  ( $m/z$  248.98), and  $\text{AuCNS}^-$  ( $m/z$  254.94) decreased after activation. In comparison, those of  $\text{Au}^{35}\text{Cl}^-$  ( $m/z$  231.94),  $\text{AuH}^{35}\text{Cl}^-$  ( $m/z$  232.94),  $\text{Au}^{35}\text{Cl}_2^-$  ( $m/z$  266.91) and  $\text{Au}^{35}\text{Cl}^{37}\text{Cl}^-$  ( $m/z$  268.91) ions increased after activation.

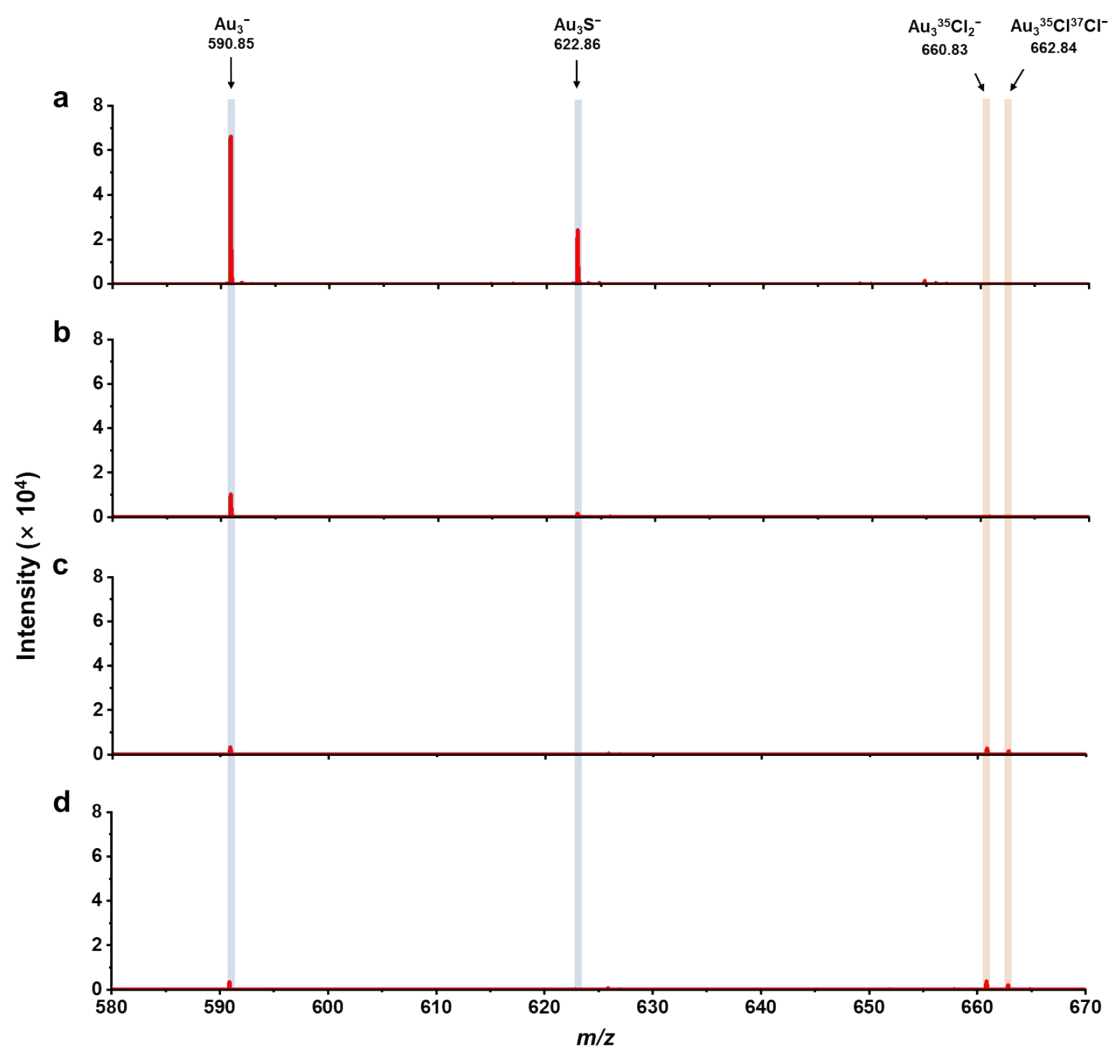


**Figure S5.** The representative ToF-SIMS spectra in the mass range of 580-670 obtained at surfaces of the freshly polished gold electrodes before (a) and after (b-d) being electrochemically treated in 0.37 M HCl for 5 (b), 15 (c), and 25 (d) segments. The signal intensities of  $\text{Au}_3^-$  ( $m/z$  590.85) ion and  $\text{Au}_3\text{S}^-$  ( $m/z$  622.86) decreased after activation. In comparison, those of  $\text{Au}_3^{35}\text{Cl}_2^-$  ( $m/z$  660.83) and  $\text{Au}_3^{35}\text{Cl}^{37}\text{Cl}^-$  ( $m/z$  662.84) ions increased after activation.

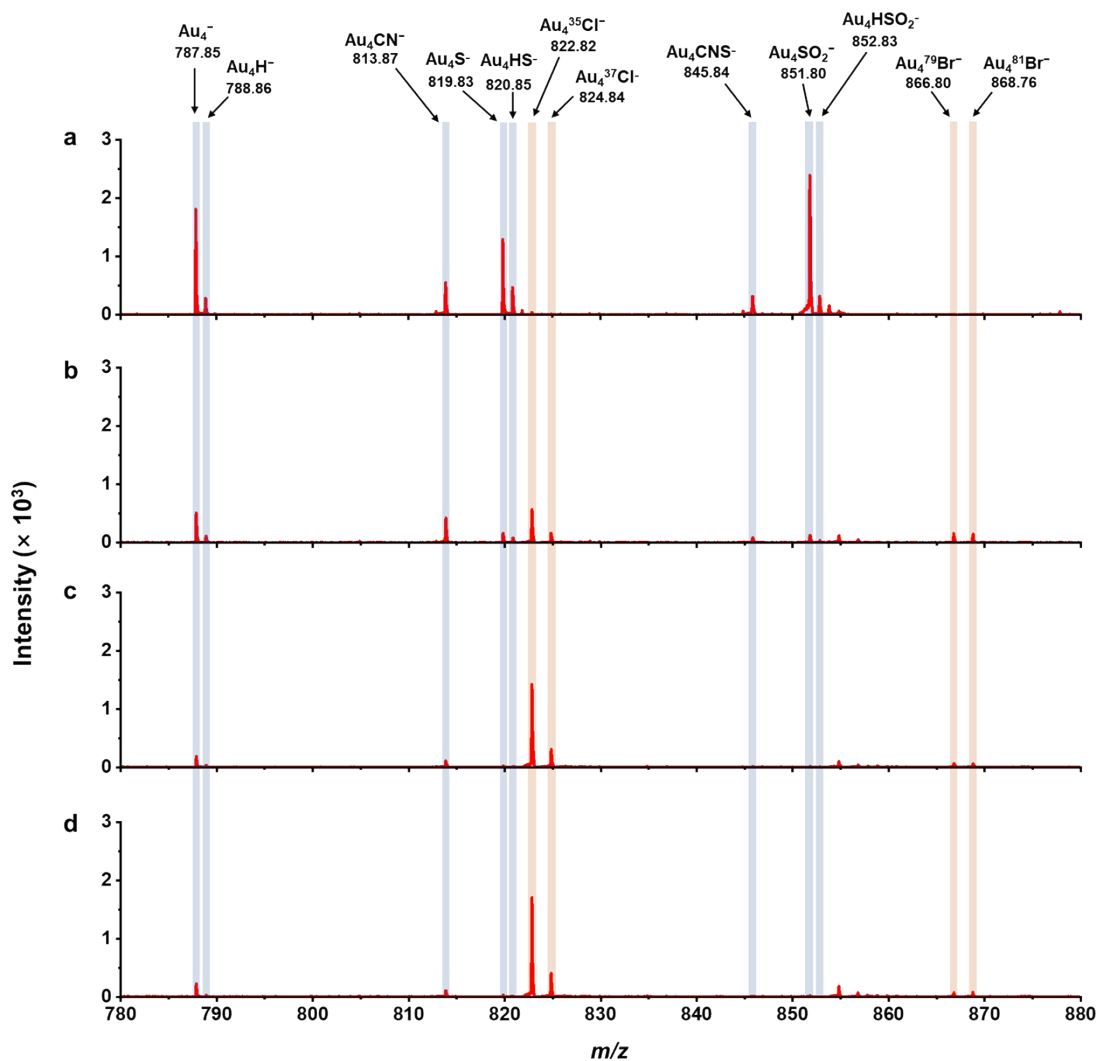


**Figure S6.** The representative ToF-SIMS spectra in the mass range of 780-880 obtained at surfaces of the freshly polished gold electrodes before (a) and after (b-d) being electrochemically treated in 0.37 M HCl for 5 (b), 15 (c), and 25 (d) segments. The signal intensities of  $\text{Au}_4^-$  ( $m/z$  787.85) ion and ions from surface contaminants including  $\text{Au}_4\text{H}^-$  ( $m/z$  788.86),  $\text{Au}_4\text{CN}^-$  ( $m/z$  813.87),  $\text{Au}_4\text{S}^-$  ( $m/z$  819.83),  $\text{Au}_4\text{HS}^-$  ( $m/z$  820.85),  $\text{Au}_4^{35}\text{Cl}^-$  ( $m/z$  822.82) and  $\text{Au}_4^{37}\text{Cl}^-$  ( $m/z$  824.84) ions significantly increased after activation. In comparison, those of  $\text{Au}_4\text{CNS}^-$  ( $m/z$  845.84),  $\text{Au}_4\text{SO}_2^-$  ( $m/z$  851.80) and  $\text{Au}_4\text{HSO}_2^-$  ( $m/z$  852.83) decreased after activation.

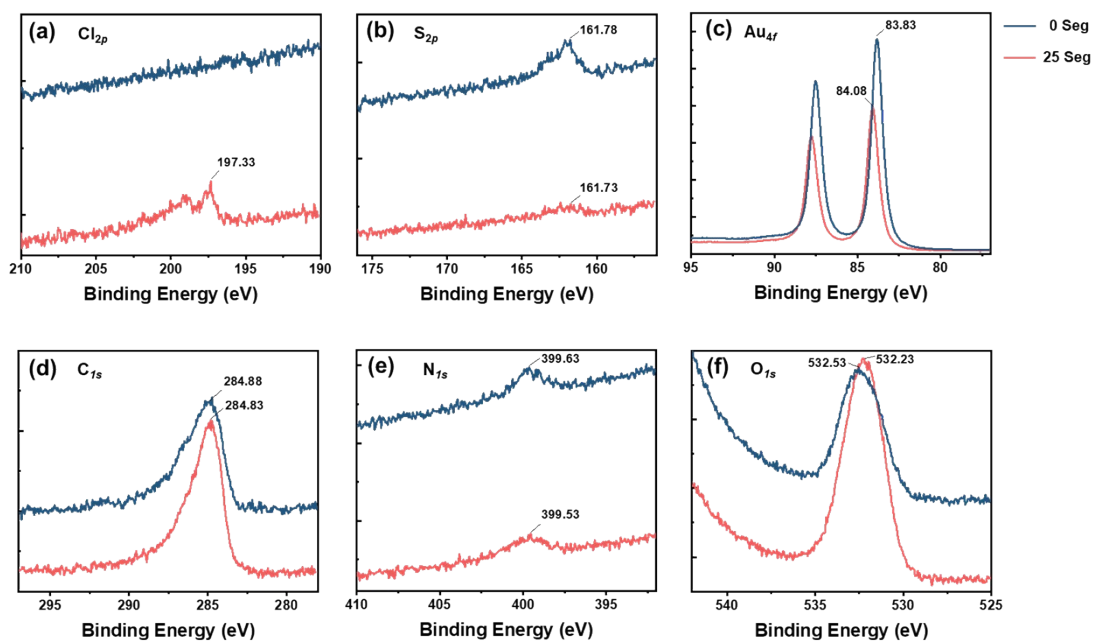


**Figure S7.** A representative group of XPS spectra of the freshly polished gold electrodes before (blue lines) and after being activated in 0.37 M HCl solution (red lines) for 25 segments: (a)  $\text{Cl}_{2p}$  peak; (b)  $\text{S}_{2p}$  peak; (c)  $\text{Au}_{4f}$  peak; (d)  $\text{C}_{1s}$  peak; (e)  $\text{N}_{1s}$  peak; (f)  $\text{O}_{1s}$  peak. We conducted XPS analysis on three independently prepared electrode surfaces to check the data repeatability and the average values of the XPS quantitative analysis data were listed in Table S1.

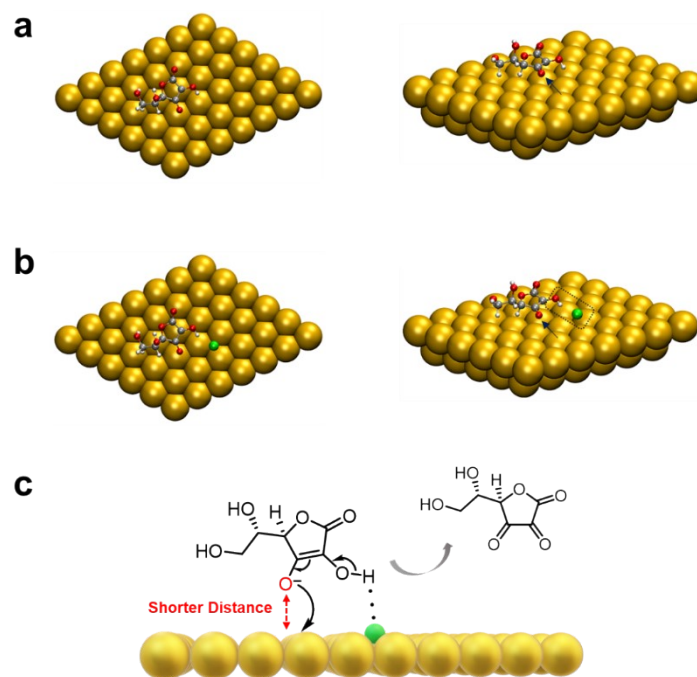


**Figure S8.** Optimized geometries of ascorbate on gold surfaces with (a) or without (b) adsorbed Cl<sup>-</sup>. Top view (left column) and side view (right column). Yellow, Au; grey, C; white, H; red, O; green, Cl<sup>-</sup>. (c) Schematic diagram of the electrochemical oxidation reaction pathway of ascorbate in the 50 mM NaNO<sub>3</sub> solution on the Cl modified gold electrode surface. The BEs in the corresponding optimized geometries are calculated to be 40.79 kcal/mol in the absence of Cl<sub>ads</sub> (Figure S7a) and 39.46 kcal/mol in the presence of Cl<sub>ads</sub> (Figure S7b), respectively, indicating a slight difference in the BE caused by the adsorbed Cl. However, in the presence of Cl<sub>ads</sub> on the gold cluster surface, one can surprisingly see a hydrogen bonding between -O-H of ascorbate and the adsorbed chloride in the optimized structure (as highlighted in the dotted box in Figure S7b). The hydrogen bonding stabilizes the ascorbate on the Cl-adsorbed gold surface. The distance between the reactive -O<sup>-</sup> of ascorbate (as pointed by the arrow in Figures S7a-b and highlighted in the reaction pathway in Figure S7c) and the plane of the first layer of gold atoms was shortened from 2.96 Å without Cl<sub>ads</sub> (Figure S7a) to 2.65 Å with Cl<sub>ads</sub> (Figure S7b), which most likely facilitated the electron transfer between ascorbate and the Cl<sub>ads</sub> modified gold electrode surface during the electro-oxidation reaction of ascorbate as shown in Figure S7c.

**Table S1.** XPS quantitative analysis results (n=3) on the polished gold electrode surfaces before (0-Seg) and after activation (25 Seg) by HCl

	$Cl_{2p}$	$S_{2p}$	$Au_{4f}$	$C_{1s}$	$N_{1s}$	$O_{1s}$
0 Seg	/	2.16% ±	59.54% ±	25.58% ±	1.82% ±	10.89% ±
		0.10%	4.23%	3.26%	0.35%	0.74%
25 Seg	1.40% ±	0.57% ±	41.16% ±	35.40% ±	2.10% ±	19.37% ±
	0.18%	0.06%	2.39%	1.20%	0.13%	2.69%

**Table S2.** Ion peaks detected on the polished gold electrode surfaces before and after activation by HCl

<i>m/z</i> (observed)	<i>m/z</i> (calculated)	dev (ppm)	Possible Assignment
25.0096	25.0073	91.97	C <sub>2</sub> H <sup>-</sup>
26.0061	26.0025	138.45	CN <sup>-</sup>
31.9736	31.9715	65.68	S <sup>-</sup>
32.9804	32.9794	30.32	HS <sup>-</sup>
34.9728	34.9683	128.69	<sup>35</sup> Cl <sup>-</sup>
36.9687	36.9654	89.27	<sup>37</sup> Cl <sup>-</sup>
41.0157	41.0134	56.08	HCN <sub>2</sub> <sup>-</sup>
41.9986	41.9974	28.57	CNO <sup>-</sup>
45.0012	44.9971	91.12	CHO <sub>2</sub> <sup>-</sup>
57.9767	57.9746	36.22	CNS <sup>-</sup>
63.9586	63.9614	43.78	SO <sub>2</sub> <sup>-</sup>
66.0147	66.0087	90.90	C <sub>2</sub> N <sub>3</sub> <sup>-</sup>
78.9206	78.9178	35.48	<sup>79</sup> Br <sup>-</sup>
79.9583	79.9563	25.01	SO <sub>3</sub> <sup>-</sup>
80.9163	80.9157	7.415	<sup>81</sup> Br <sup>-</sup>
96.9635	96.9590	46.41	HSO <sub>4</sub> <sup>-</sup>
196.9673	196.966	6.600	Au <sup>-</sup>
222.9707	222.9691	7.176	AuCN <sup>-</sup>
223.9745	223.9765	8.930	AuHCN <sup>-</sup>
228.9384	228.9381	1.310	AuS <sup>-</sup>
231.9363	231.9349	6.036	Au <sup>35</sup> Cl <sup>-</sup>
232.9421	232.9427	2.576	Au <sup>37</sup> Cl <sup>-</sup>
248.9753	248.9722	12.45	AuC <sub>2</sub> N <sub>2</sub> <sup>-</sup>
254.9404	254.9411	2.746	AuCNS <sup>-</sup>
257.9425	257.9379	17.83	AuCN <sup>35</sup> Cl <sup>-</sup>
259.9330	259.9355	9.618	AuCN <sup>37</sup> Cl <sup>-</sup>
266.9119	266.9037	30.72	Au <sup>35</sup> Cl <sub>2</sub> <sup>-</sup>
268.9077	268.9008	25.66	Au <sup>35</sup> Cl <sup>37</sup> Cl <sup>-</sup>

310.8618	310.8532	27.67	$\text{Au}^{35}\text{Cl}^{79}\text{Br}^-$
312.8584	312.8511	24.29	$\text{Au}^{37}\text{Cl}^{79}\text{Br}^-$
393.9218	393.9326	27.42	$\text{Au}_2^-$
394.9396	394.9409	3.292	$\text{Au}_2\text{H}^-$
419.9291	419.9356	15.48	$\text{Au}_2\text{CN}^-$
425.9010	425.9046	8.452	$\text{Au}_2\text{S}^-$
426.9106	426.9125	4.450	$\text{Au}_2\text{HS}^-$
428.8992	428.9014	5.129	$\text{Au}_2^{35}\text{Cl}^-$
430.8900	430.8985	19.73	$\text{Au}_2^{37}\text{Cl}^-$
451.8994	451.9077	18.37	$\text{Au}_2\text{CNS}^-$
590.8524	590.8991	79.03	$\text{Au}_3^-$
622.8573	622.8712	22.32	$\text{Au}_3\text{S}^-$
660.8349	660.8339	1.81	$\text{Au}_3^{35}\text{Cl}_2^-$
662.8351	662.8339	15.86	$\text{Au}_3^{35}\text{Cl}^{37}\text{Cl}^-$
787.8532	787.8657	15.86	$\text{Au}_4^-$
788.8621	788.8740	15.08	$\text{Au}_4\text{H}^-$
813.8736	813.8687	6.021	$\text{Au}_4\text{CN}^-$
819.8332	819.8377	5.489	$\text{Au}_4\text{S}^-$
820.8455	820.8456	0.122	$\text{Au}_4\text{HS}^-$
822.8200	822.8345	17.62	$\text{Au}_4^{35}\text{Cl}^-$
824.8400	824.8316	10.18	$\text{Au}_4^{37}\text{Cl}^-$
845.8411	845.8408	0.3547	$\text{Au}_4\text{CNS}^-$
851.7961	851.8276	36.98	$\text{Au}_4\text{SO}_2^-$
852.8279	852.8354	8.794	$\text{Au}_4\text{HSO}_2^-$
866.8029	866.7840	21.80	$\text{Au}_4^{79}\text{Br}^-$
868.7637	868.7820	21.06	$\text{Au}_4^{81}\text{Br}^-$

---